JOURNAL OF MATERIALS SCIENCE 13 (1978) 647–656

Estimation of remaining creep life of an aluminium alloy from creep crack density measurements

R. N. WILSON
Materials Department, Royal Aircraft Establishment, Farnborough, Hants, UK

Long transverse test pieces of fully aged RR58 plate were stressed in tension at 278 and 308 MPa at 120° C for various fractions of their creep lives. The test pieces were subsequently sectioned, mechanically and electrolytically polished and the numbers of cracks per square millimetre were measured by optical microscopy. The crack density, n, increased linearly with creep strain ϵ at both stress levels. No accurate assessment of the variation of n with time was possible. Good agreement between the crack densities measured on duplicate microsections was achieved when the crack density was greater than 10 cracks mm^{-2}. The crack densities in the uniformly strained portions of 11 test pieces from the same plate, fractured at 150° C at stresses within the range 200 to 290 MPa were also measured. The crack density decreased from 45 cracks mm^{-2} at 200 MPa to 4 cracks mm^{-2} at 290 MPa. A regression equation $n/\epsilon = 164 - 0.57\sigma$ (where σ is the applied stress) was derived assuming linear n versus ϵ relationships at 150° C. The 90% confidence limits were derived for the determination of an unknown stress level from a single measurement of n/ϵ. Of the creep life prediction methods discussed, only the correlation of creep crack density and creep strain is of sufficient accuracy and this only when the creep stress and creep temperature are low, i.e. only for those conditions which would develop a high crack density at small fractions of the creep life.

1. Introduction

The rates at which creep cracks nucleate and grow in an alloy under stress are not only of fundamental interest in the study of the creep phenomenon but are also of technological importance since they affect the life of a component in service.

Dyson and McLean [1, 2] have proposed that the extent of cavitation during creep could be used to estimate the remaining life of a component in service. They showed that, for Nimonic 80A stressed in tension at 750° C, the number of cracks mm^{-2}, n, increased approximately linearly with strain, ϵ, up to 75% of the creep life t_f. The crack density at fracture only varied by a factor of two over the stress range 154 to 385 MPa and these workers also suggested that the technique may be applicable to components subjected to variable service stresses. The slopes n/ϵ were different for different stresses, a high n/ϵ value being associated with poor ductility to fracture.

Similar tests at RAE on fully aged unclad RR58 sheet [3, 4] also showed that the creep crack density, measured on electropolished microsections, increased linearly with creep strain although the crack densities measured were an order of magnitude lower than those reported for the Nimonic 80A alloy. Increased uncertainty in the measurements for the RR58 alloy existed because of the complex microstructure, which contained cracked particles, porous regions and regions of overheating, and this, combined with the low crack densities, could prevent the technique being applied successfully to this alloy. Dyson and McLean [1, 2] did not consider separately the relationships between n and t and between n and ϵ because they were similar for times up to 75% of t_f. However in practice it is

usual to know the time a component has been in service rather than the strain it has undergone and therefore the relationship between n and t would be the more convenient one to use. The exact procedure was not defined by Dyson and McLean perhaps because, once the crack density has been measured it can be utilized in one of several ways. In the simplest case the n versus t/t_f curve is common for a range of stresses at a given temperature [2] and therefore measurement of n after a known time would determine t/t_f and hence the remaining life. However if a common n versus t/t_f curve does not exist for different stresses then the slopes n/t (or n/ϵ) for various stresses would be required from laboratory tests. The service component would be inspected after two intervals of time (or strain), n/t determined and hence the creep stress derived. The remaining service life would be obtained by reference to laboratory stress–rupture data.

The application of the above predictive methods will be considered in this paper. The work reported was undertaken to determine whether or not these methods could be applied to the complex precipitation hardened aluminium alloy plate RR58.

Four factors have been examined: (a) the minimum fraction of the creep life at which creep cracks could be detected by optical microscopy, (b) the accuracy of the crack density measurements, (c) the relationships between crack density and creep time and strain, and (d) the feasibility of applying the above methods to the prediction of the remaining life of a component made of RR58 plate.

2. Material and experimental techniques

The 3 in. thick, fully aged, stretched RR58 alloy plate was manufactured by James Booth Aluminium Co. The composition (wt %) quoted on the release note was:

Cu	Mg	Mn	Fe	Si
2.45	1.43	0.11	1.01	0.18
Zn	Ti	Ni	Al	
0.09	0.03	1.27	Balance	

Fracture toughness (K_{Ic}) and tensile data (single test pieces) for an adjacent piece of plate were determined and are given below:

		Longitudinal	Long Trans.	Short Trans.
0.2% PS	MPa	406	391	377
TS	MPa	432	435	425
El%	(on $4\sqrt{A}$)	10	9	7.5
K_{Ic}	MPa $\sqrt{m}$	23.5 (*L/T*)	21.0 (*T/L*)	18.5 (*ST/L*)

Long transverse round bar creep test pieces with $\frac{1}{2}$ in. BSF threaded ends, Fig. 1, were machined from the near surface region of one face of the plate. The gauge lengths of the test pieces were scribed so that creep strains could be determined by a travelling microscope after the tests had been terminated. An equivalent gauge length extensometer (i.e. an extensometer attached to the shoulders of the test piece and previously calibrated to measure the deformation in the gauge length of the test piece) was fitted to those test pieces tested to failure. Stress levels 278 and 308

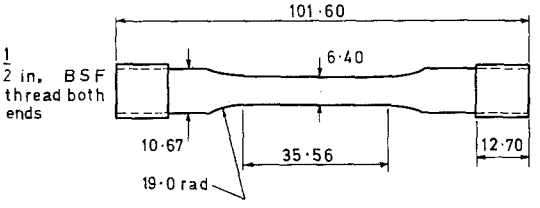

Figure 1 Dimensions of round bar creep tests piece (mm) used with equivalent gauge length extensometer.

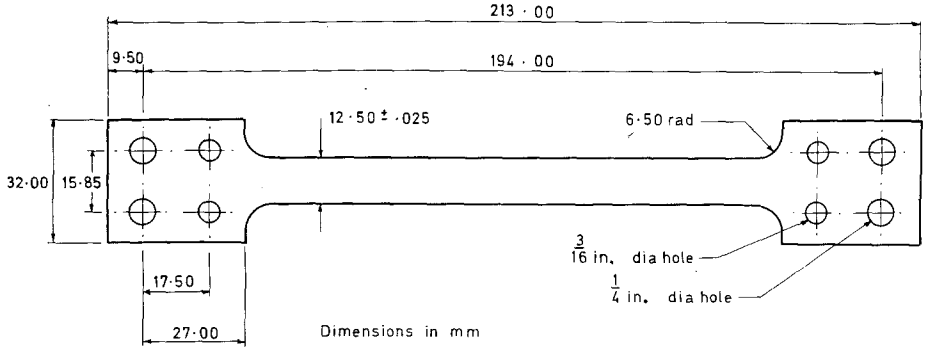

Figure 2 Dimensions of strip test piece 1.69 mm thick.

MPa at 120° C were selected to give estimated times to fracture of 20 000 and 3000 h in a constant load machine. Six test pieces were stressed at 308 MPa and four at 278 MPa and tests were shut down at various fractions of their creep lives.

A second series of eleven long transverse BNF strip test pieces Fig. 2 from another piece of the same plate had been fractured at 150° C at stresses in the range 200 to 290 MPa. The creep ductilities recorded for these tests were the last recorded extensometer readings (extensometer attached to gauge length of test piece).

Microsections from all test pieces were cut in the long transverse/short transverse plane (relative to the plate). An illustration of the sectioning of the round bar test piece is shown in Fig. 3. The microsections were mechanically polished to 0.25 μm diamond finish using selvyt cloth and hyprez fluid, followed by electropolishing for 10 sec at 70° C in Lenoirs solution (a chromic–sulphuric–phosphoric acid solution). This solution was selected because it produces a minimum of etching and leaching-out of particles and has been widely used for the preparation of thin foils for transmission electron microscopy.

The crack density, n, cracks mm^{-2} in a test piece was determined by counting the number of cracks when the microsection was scanned in the short transverse direction using the optical microscope at × 500 magnification, i.e.

$$n = N/lw \text{ cracks mm}^{-2}$$

where N = number of cracks, l = length of traverse, w = width of traverse (0.18 mm) i.e. the width defined by the eye piece graticule on the surface of the specimen.

The microsections were scanned at 1 mm intervals along the length of the test piece and a mean crack density and standard deviation calculated. Duplicate microsections were prepared from the round test pieces. The fracture surfaces of all broken test pieces were examined by scanning electron microscopy. The faceted areas on the fractured BNF test pieces were measured as a fraction of the total area. This technique has been described elsewhere. [3].

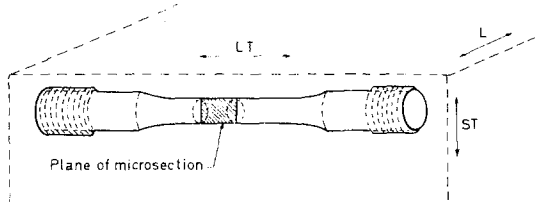

Figure 3 Diagram showing the orientation of the microsection of the test piece to the original plate.

3. Results

3.1. Relationships between crack density and creep strain and creep time at constant stress at 120° C

Ten round bar creep test pieces were tested at 120° C, six of which were stressed at 308 MPa and four at 278 MPa. The tests were shut down after predetermined fractions of their creep lives as shown in Table I. Two microsections were prepared from each test piece designated Series I and Series II, in order to estimate the reproducibility of the specimen preparation technique and the repeatability of the crack density measurements. The results are presented in Table II. Creep cracks were detected in all test pieces, i.e. creep cracks were present after 20% of the time to fracture at 308 MPa and after 30% at 278 MPa at 120° C. The cracks were formed on grain boundaries lying approximately normal to the applied tensile stress. Fig. 4 shows plots of the average crack density derived from all measurements from both series versus the creep strain. The plots show a linear dependence of crack density upon creep strain at both stresses. The rates of accumulation of creep cracks with creep strain were very different at the two stresses, the slopes n/ϵ being 73 at 278 MPa and 2.5 at 308 MPa. Unfortunately the range of crack density measurements determined at the higher stress level was comparable to the mean crack density, resulting in low confidence in the position of the line. This is shown by a com-

TABLE I round bar test pieces stressed at 278 and 308 MPa at 120° C

Test piece no.	Creep stress (MPa)	Test duration (h)	Creep strain (%)	Shut down or fractured
5	308	505	0.78	sd
3	308	1055	1.44	sd
12	308	1801	2.65	sd
10	308	1990	2.15	sd
1	308	2653	7.14*	f
11	308	3432	1.67	sd
8	278	6935	0.47	sd
2	278	9995	1.01	sd
7	278	13000	0.67	sd
6	278	21717	1.19	f

*Uniform elongation 5.6%.

TABLE II Crack density measurements on round bar test pieces stressed at 278 and 308 MPa at 120° C

Test piece no.	Crack density measured on individual traverses (no. mm^{-2})	Average density (no. mm^{-2})	Standard deviation
	Series I		
5	4.0, 3.2, 4.0, 7.9, 4.8, 7.3, 3.2, 3.2	4.7	1.9
3	3.0, 4.5, 1.8, 2.7, 2.7	3.0	1.0
12	8.9, 13.1, 10.2, 11.7, 7.9, 9.5, 8.6, 9.7, 7.3	9.6	1.8
10	8.9, 7.3, 7.9, 7.3, 7.1, 5.6, 5.6, 9.7, 11.1	7.8	2.0
1	15.3, 12.3, 25.4, 20.8, 12.1, 19.4, 18.9, 5.0	16.1	6.4
11	5.6, 11.1, 1.6, 7.1, 7.9, 4.7, 8.7, 10.3	7.1	2.9
8	8.7, 10.3, 4.0, 8.5, 7.9, 5.6, 7.3, 5.6, 7.9, 6.3	7.2	1.9
2	48.4, 45.9, 32.0, 37.9, 46.8, 33.6, 44.3	41.2	6.6
7	19.3, 21.0, 28.9, 24.6, 33.3, 23.7, 20.2, 19.3	23.2	4.8
6	37.3, 69.0, 63.5, 55.6, 77.8, 69.8, 73.0	63.7	13.6
	Series II		
5	1.0, 1.0, 2.0, 3.0, 2.0	1.8	0.8
3	1.7, 0.9, 0.9, 0.9, 3.4, 1.7, 4.2, 5.1, 1.7, 1.7,	2.2	1.5
12	6.9, 3.8, 3.1, 3.1, 3.8, 8.5	3.7	2.3
10	3.4, 6.8, 5.1, 1.8, 5.2, 2.7, 6.3, 7.8	4.2	2.1
1	18.0, 22.0, 14.4, 13.6, 12.0	15.8	3.6
11	4.2, 2.1, 4.5, 5.3, 3.5, 2.5, 1.7	1.7	1.3
8	10.9, 9.1, 4.5, 14.3, 4.3, 8.7, 2.1, 14.3, 4.8, 6.3	7.9	4.2
2	56.1, 49.0, 37.8, 35.7, 27.1, 43.6, 25.0	39.1	11.3
7	21.4, 26.2, 19.0, 30.2, 26.6, 16.4	23.3	5.0
6	72.4, 76.7, 85.3, 77.1, 67.8, 56.7, 57.6, 55.1, 38.1, 59.3	64.6	13.9

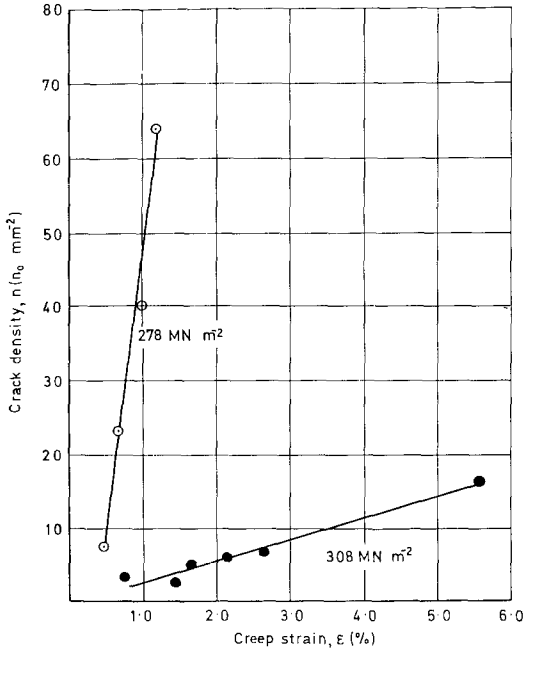

Figure 4 Relation between creep crack density and creep strain at 120° C at 278 MPa and 308 MPa. Mean values of series I and II measurements.

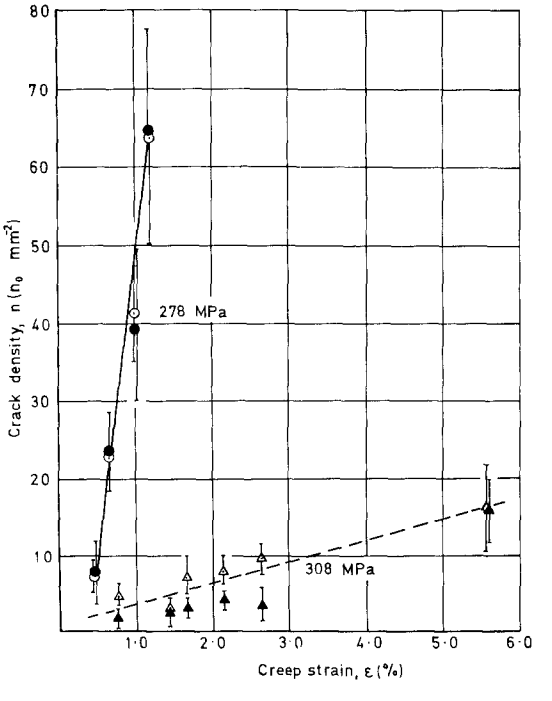

Figure 5 As Fig. 4 but showing means of series I (open symbols) and series II (solid symbols) measurements with standard deviations.

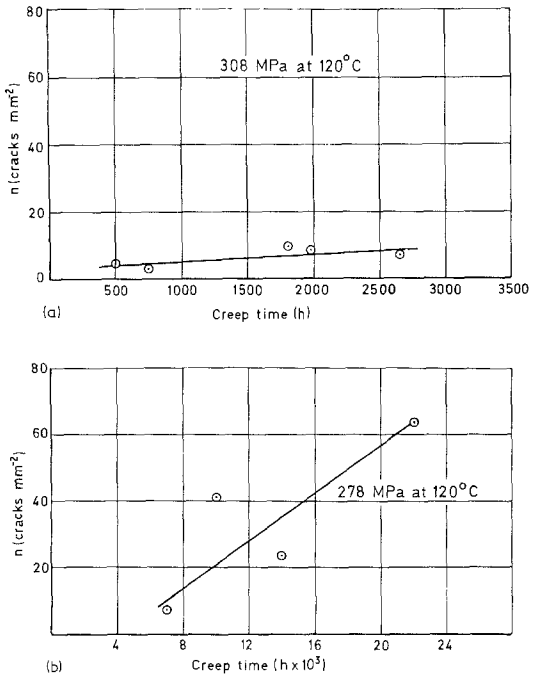

Figure 6 Relation between creep crack density and creep time at 120° C for (a) 308 MPa and (b) 278 MPa. Mean values of series I and II measurements.

parison of the results from duplicate microsections plotted separately in Fig. 5. The bars are the standard deviations from Table II. However agreement between the measurements of Series I and Series II for the test pieces stressed at 278 MPa was good. The statistical significance of these measurements will be discussed in Section 4.

Fig. 6a and b shows the relation between n and creep time for 308 and 278 MPa at 120° C. It can be seen that the accuracy of any relationship between n and t is poor. Fig. 7 shows n versus fractional time to failure for the two stress levels.

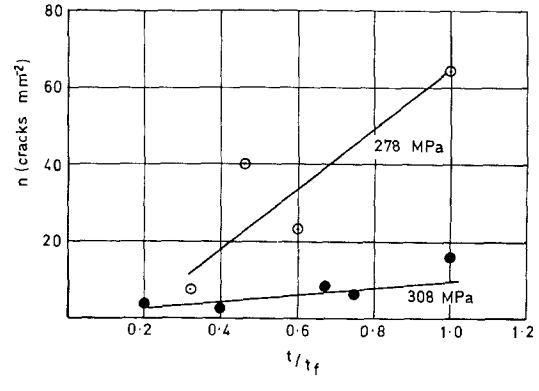

Figure 7 Relation between crack density and fractional time to failure at 120° C. ○ 278 MPa, ● 308 MPa.

Not only does the scatter remain but also the results fall into two distinct groups. Thus the observation of Dyson and McLean [2] that a common n versus t/t_f curve exists over a wide stress range for the Nimonic 80A alloy does not apply to the precipitation hardened RR58 alloy.

TABLE III Strip test pieces fractured at 150° C (ϵ_f values are the last recorded extensometer strains)

Test piece no.	Creep stress (MPa)	Fracture strain ϵ_f (%)	Time to fracture (h)
1B5	290	3.8	76
1B4	280	2.16	129
1B6	276	2.48	250
8A6	276	2.22	334
1B7	270	1.69	339
1B3	260	1.92	630
1B2	240	1.18	1376
1B1	240	1.26	1559
1B8	230	1.30	2347
8A2	230	1.15	2087
6B4	200	0.84	4978

3.2. Relationship between crack density at fracture and stress at 150° C

The creep test results for eleven BNF strip test pieces fractured at 150° C are shown in Table III. The test pieces were fractured as part of a Structures Department RAE test programme. The fracture surfaces of all the test pieces were examined by optical and scanning electron microscopy. Since the creep cracks occurred on grain boundaries lying approximately normal to the tensile stress, the area fraction of the fracture surface which was in the form of intercrystalline facets was measured. This fraction increased with lower applied stress as shown in Fig. 8. An example of a fracture facet is shown at A in Fig. 9.

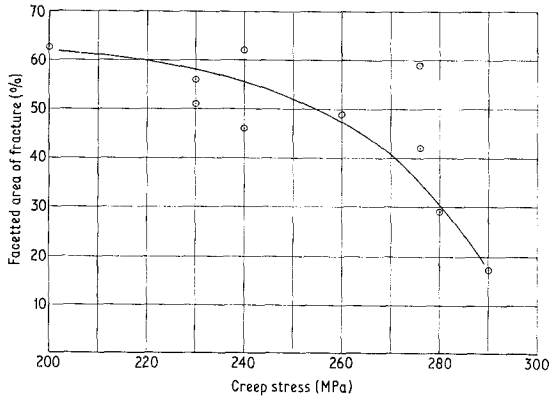

Figure 8 The relation between the creep stress at 150° C and the percentage faceted area on the fracture surface.

The gauge lengths of the test pieces were sectioned and polished as described earlier. The crack densities were measured by individual traverses across the microsections and are shown in Table IV. The plot of the mean crack density versus creep stress is shown in Fig. 10. The crack density increased with decreasing stress, from 3.4 cracks mm^{-2} at 290 MPa up to 44.8 cracks mm^{-2} at 200 MPa. An example of a microsection

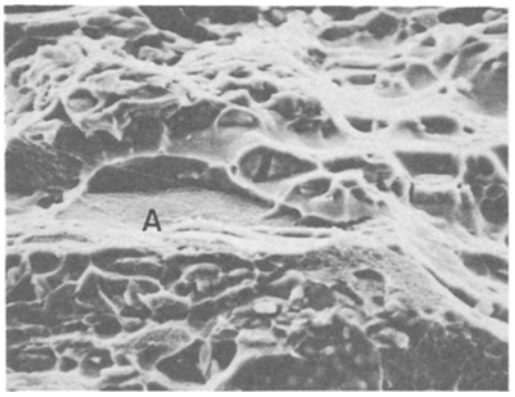

Figure 9 Test piece 6B4 fractured at 200 MPa at 150° C showing fracture facet, A (× 700).

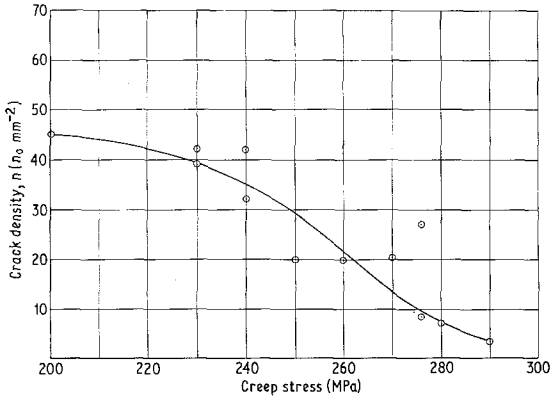

Figure 10 The relation between the creep stress at 150° C and the creep crack density.

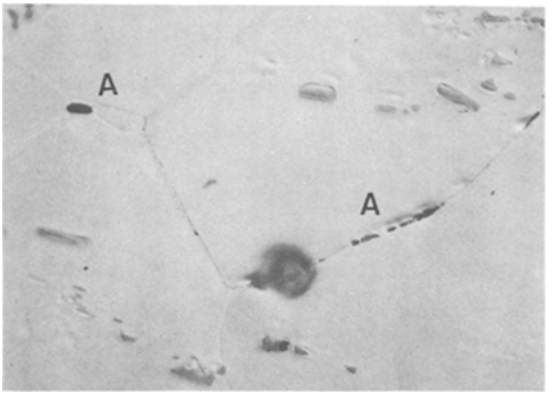

Figure 11 Test piece 1B5 fractured at 290 MPa at 150° C. Electropolished microsection showing grain boundary cracks, A (× 650).

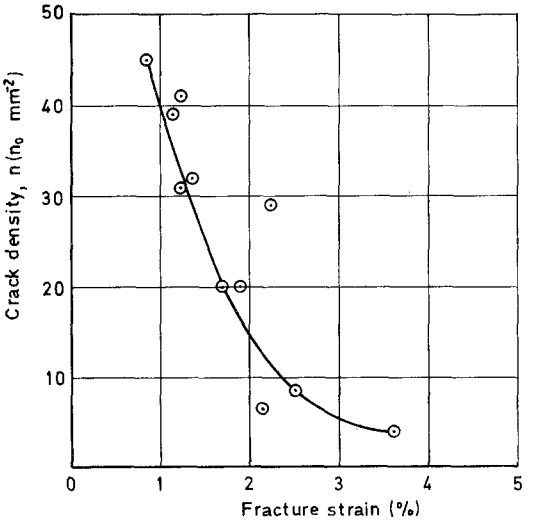

Figure 12 Relation between creep crack density and strain at fracture for test pieces fractured at 150° C.

TABLE IV Crack density measurements on strip test pieces fractured at 150° C

Test piece no.	Crack density measured on individual traverses (no. mm^{-2})	Average density (no. mm^{-2})	Standard deviation
1B5	3.4, 4.5, 3.4, 3.4, 2.2	3.4	0.81
1B4	3.4, 6.7, 6.7, 10.0, 6.7,	6.7	2.3
1B6	6.7, 9.0, 11.2, 7.8, 7.8	8.5	1.7
8A6	25.8, 31.4, 25.8, 29.1, 26.9	27.8	4.5
1B7	20.2, 23.5, 20.2, 28.0, 16.8, 19.0,	21.3	3.9
1B3	16.8, 20.1, 25.8, 22.4, 17.9, 14.5, 22.4	19.9	4.0
1B2	51.5, 42.6, 26.3, 60.4	45.2	14.5
1B1	26.9, 32.5, 32.5, 30.5, 41.1, 24.9	31.4	5.6
1B8	29.1, 30.2, 29.1, 34.7, 37.0	32.0	3.6
8A2	50.4, 34.7, 28.6, 52.6	41.6	11.8
6B4	40.3, 45.9, 47.0, 34.7, 56.0, 56.0	46.6	8.5

showing small grain boundary creep cracks, A, can be seen in Fig. 11. The plots of crack density versus creep fracture strain and versus time to fracture are shown in Figs. 12 and 13 respectively.

Assuming a similar linear dependence of n with ϵ at constant stress at 150° C as was observed for the alloy at 120° C, it is possible to calculate n/ϵ values for each of the eleven test pieces and derive a relationship between n/ϵ and the applied stress from the values of n/ϵ at fracture. The results are plotted in Fig. 14. The relationship was approximately linear and the regression equation to the line using the principle of least squares was

$$n/\epsilon = 164 - 0.57\sigma.$$

The n/ϵ values for the two stress levels at 120° C

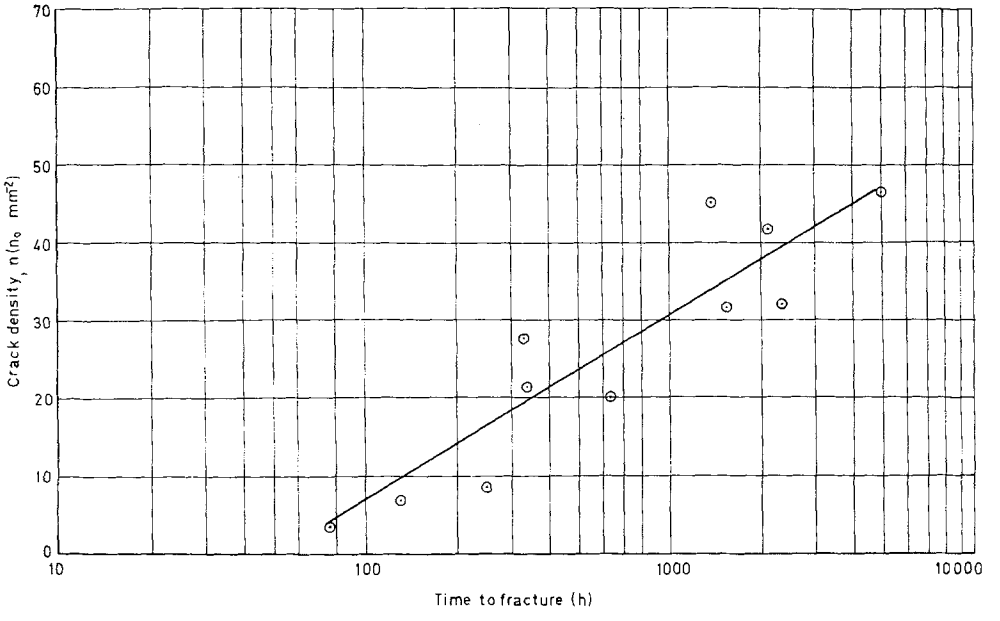

Figure 13 Relation between the crack density and log time to fracture at 150° C.

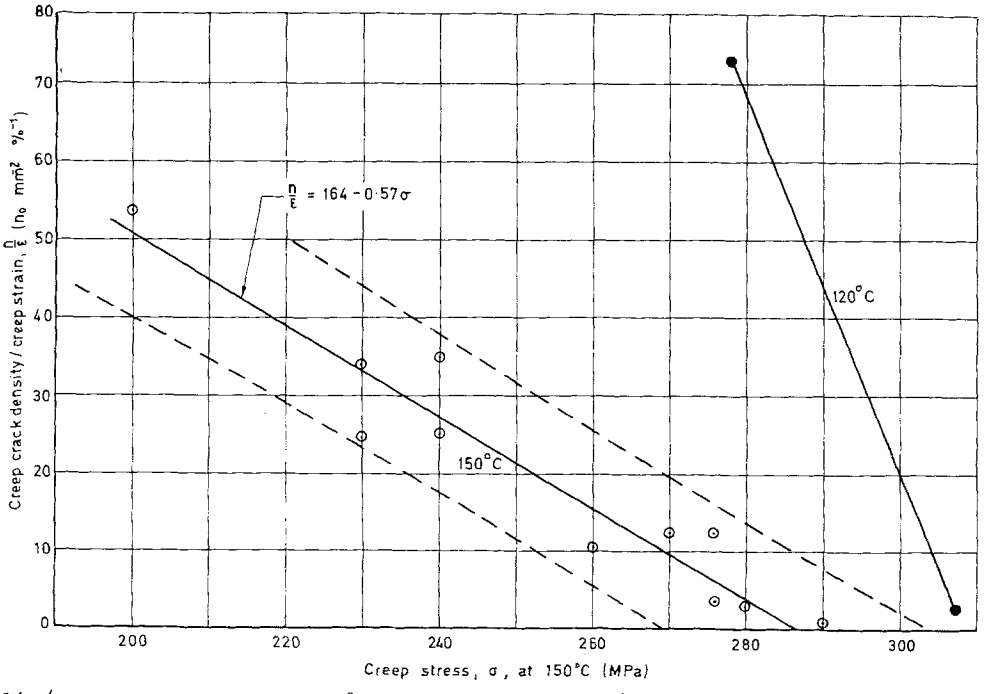

Figure 14 n/ϵ versus creep stress, σ, at 150° C showing regression line $n/\epsilon = 164 - 0.57\,\sigma$. Dashed lines show 90% confidence limits for σ, for any single measurement of n/ϵ, n/ϵ values at 120° C are also included.

are also included in Fig. 14 and the equation joining these two points is

$$n/\epsilon = 725 - 2.35\sigma$$

indicating that the n/ϵ versus σ relationship changed rapidly with temperature.

4. Discussion

Hiduminium RR58 is a complex precipitation hardened aluminium alloy, the microstructure containing large (>1 μm diameter) insoluble particles of $FeNiAl_9$ with some particles of Al_6Cu_3Ni, Cu_2FeAl_7, $Al_4CuMg_5Si_4$ and Mg_2Si [5]. Some of these particles may have been cracked during the manufacture of the plate and others may be associated with porosity. Localized overheating may also be present and cause further porosity [6]. These features existing from the unstressed microstructure make the precise measurement of the creep crack density difficult particularly when the density of creep cracks is low.

The proposal by Dyson and McLean [1, 2] to use creep crack density measurements as a means of predicting the remaining creep life was based upon the observations that in Nimonic 80A the crack density n varied linearly with creep strain ϵ, that n versus t/t_f curve was common to a range of stress levels, and that the slope n/ϵ was a simple function of stress and temperature. They suggested therefore that a component could be taken out of service or examined *in situ* and on determining the value of n, the creep strain undergone and its remaining life could be established, assuming that the stress σ, time and temperature were known.

The present results on the creep cracking of RR58 plate indicate that an approximately linear relationship exists between measured creep crack density and creep strain and that the slope n/ϵ varies with applied stress at 120° C. Furthermore, if this linear dependence also occurs at 150° C then the crack density measurements on the fractured test pieces indicate that the slope n/ϵ changes in a simple manner with applied stress.

Dyson and McLean have shown that for the Nimonic 80A alloy a plot of crack density n against fractional time to failure t/t_f approximates to a common curve over a wide stress level. This relationship has not been observed in the present work, the rate of crack formation as a function of fractional time to failure differing greatly for the stress levels 278 and 308 MPa at 120° C. The scatter of crack density measurements with creep time was also disappointingly large, such that this relationship could not be used with confidence for predicting creep life.

The means and variances of the crack densities in the duplicate microsections of the test pieces stressed at 120° C have been analysed by elementary statistics [7, 8]. The student 't' test has been applied to determine whether the mean values from the duplicate microsections were significantly different, and the F test has been used to determine the significance of the differences between their variances. The analyses indicated that the means and variances of the duplicate microsections could be considered as being from the same population (to 95% confidence level) for all test pieces stressed at 278 MPa. However in all but one test pieces at 308 MPa the means were not similar to this degree of confidence due primarily to the lower crack densities measured in these test pieces. Almost identical results were obtained when the F test was applied to the differences between the variances of the individual microsections. Again the duplicate microsections of test pieces stressed at 278 MPa were similar, to 95% confidence level, whereas those stressed at 308 MPa were not. The analyses indicate that the experimental technique was satisfactory for test pieces stressed at 278 MPa where the crack densities developed during tests were high. For test pieces stressed at 308 MPa, however, the lower crack densities resulted in greater uncertainty in the recognition of cracks and the discrimination between these cracks and other metallurgical defects.

The linear relation between n and ϵ at constant stress, σ, and temperature, and the high degree of confidence in measurements at low applied stresses, should allow the technique to be applied to practical service problems. A regression equation of the form

$$n/\epsilon = a + b\sigma \quad \text{(where } a \text{ and } b \text{ are constants)}$$

should enable the stress to be calculated and hence, from laboratory test data, the remaining life of the component.

Davies and Goldsmith [8] have reported that where one variable e.g. σ is the independent variate and the second variable e.g. n/ϵ is dependent upon it, the regression equation derived for the dependence of n/ϵ upon σ may be used for the dependence of σ upon n/ϵ. The variance of the stress $V_{(\sigma)}$ for a given n/ϵ determination may be

derived using the equation

$$V_{(\sigma)} = S^2/b^2 \left[(1/m + 1/N) + \left(\frac{n/\epsilon - \bar{n}/\epsilon}{b} \right)^2 \frac{1}{\Sigma(\sigma - \bar{\sigma})^2} \right],$$

where m = number of new determinations made
S = standard deviation of points about regression line
b = slope of regression line
N = number of specimens measured to
$\bar{n}/\epsilon$ and $\bar{\sigma}$ are the coordinates of the centroidal point of the line.

The dashed lines in Fig. 14 are the 90% confidence limits for σ for a given measurement of n/ϵ. The limits are approximately ±20 MPa over the range of n/ϵ values studied. Although these limits may be considered unacceptably wide it should be pointed out that if more than one measurement m of n/ϵ is made then $V_{(\sigma)}$ is considerably reduced. For example if two measurements are made to determine n/ϵ then $M = 2$ and the 90% confidence limit is reduced to ±12.5 MPa and if $M = 3$ the value is ±10.5 MPa.

It should be emphasized that as shown in Fig. 14 the creep temperature could influence the n/ϵ versus σ slope and the temperature would need to be known with some accuracy before the stress levels could be estimated. Greater accuracy could have been achieved if the values of n/ϵ for each level of σ had been obtained by the procedure which had been used at 120° C (i.e. the mean slope n/ϵ from a number of test pieces) and not from the value of a single fractured test piece.

The above tests have been carried out in laboratory conditions where maximum care was exercised both during the creep testing and the preparation of the microsections. Changes to the preparation technique and even of the investigator, (which influences the decision as to what is a crack and what is not) would influence these measurements. The creep tests were at constant load and constant temperature on smooth test pieces. The effects of variable loads and temperatures and of stress concentrations upon crack density have not been studied. Before any reliability can be placed upon the crack density measurements as a means of predicting the remaining life of a component in service, these factors and also the variability in behaviour from batch to batch of material must be examined.

5. Conclusions

Optical microscopy has been used to determine creep crack densities in test pieces of RR58 alloy tested at 120 and 150° C. A linear relationship between n (number of cracks mm^{-2}) and creep strain has been found for test pieces stressed at 278 and 308 MPa at 120° C.

Creep cracks were detected in all test pieces examined, i.e. after 30% of the life at 278 MPa and 20% of the life at 308 MPa. The average values of n/ϵ at 278 and 308 MPa were 73 and 2.5 respectively (where ϵ = % creep strain).

Errors in crack density measurements arose from porosity, cracked particles and overheating in the microstructure, these errors becoming large at crack densities below $10\,mm^{-2}$. Agreement to within 95% confidence level was possible between duplicate microsections at higher crack densities.

The crack densities in test pieces fractured at 150° C at stresses within the range 200 to 290 MPa increased with reduction in the applied stress. A regression equation $n/\epsilon = 164 - 0.57\sigma$ was derived for these test pieces.

The determination of creep crack densities in RR58 alloy by optical microscopy is feasible in plain test pieces when the crack density is high (greater than $10\,mm^{-2}$) i.e. when the creep stress and temperature are low. It has been shown that the determination of the slope n/ϵ and a knowledge of the relationship between n/ϵ and stress does permit an estimate of the stress level in a component from a single measurement of n/ϵ provided the temperature is known. The accuracy of the estimate depends upon the accuracy of the n/ϵ determination for each value of stress and the number of measurements of n/ϵ on the component. The application of the technique to a practical problem would require a knowledge of how crack density varies with fluctuations in stress and temperature. The differences in creep cracking behaviour between batches of material would also require study.

Acknowledgements

The author would like to thank Mrs R. A. Whittaker and Mr L. W. Larke for carrying out the creep tests, Mr M. S. Binning and Mr C. J. Peel for many helpful discussions and Mr J. N. Webb, Structures Department, RAE, for supplying the test pieces fractured at 150° C. This paper is printed by permission of the Controller HMSO.

References

1. B. F. DYSON and D. McLEAN, NPL Report IMS44 (1971).
2. *Idem, Metal Sci. J.* 6 (1972) 220.
3. R. N. WILSON and C. J. PEEL, RAE Technical Report 73149 (1974).
4. R. N. WILSON, Conference on Practical Implications of Fracture Mechanisms (Institution of Metallurgists, 1973) p.103.
5. Mme. J. MOULIN and D. ADENIS, *Mem. Sci. Rev. Met.* 65 (1968) 505.
6. P. J. E. FORSYTH and A. C. SMALE, Unpublished MOD Report (1970).
7. A. M. NEVILLE and J. B. KENNEDY, "Basic statistical methods for engineers and scientists", (Intertext, New York, 1968) p.139.
8. O. L. DAVIES and P. L. GOLDSMITH, "Statistical methods in research and production 4th edition (Oliver and Boyd, Edinburgh, 1972) p.205.

Received 27 June and accepted 25 July 1977.